IAC–06–A3.P.3.07

ROBUST AERODYNAMIC AIRFOIL DESIGN OPTIMIZATION AGAINST WIND VARIATIONS FOR MARS EXPLORATORY AIRPLANE

Author
Koji Shimoyama*
University of Tokyo, currently, Tohoku University, Sendai, 980-8577, Japan
shimoyama@edge.ifs.tohoku.ac.jp

Co-authors
Akira Oyama† and Kozo Fujii‡
Japan Aerospace Exploration Agency, Sagamihara, Kanagawa, 229-8510, Japan
{oyama, fujii}@flab.eng.isas.jaxa.jp

Robust aerodynamic airfoil design optimizations of Mars exploratory airplane against wind variations have been carried out by using DFMOSS coupled with the CFD simulation. The present robust optimizations successfully found the airfoil designs with robust aerodynamic performances against wind variations. Obtained airfoil design information about the optimality and the robustness of aerodynamic performances indicated that an airfoil with smaller camber can improve the robustness in lift to drag ratio against the variation of flight Mach number, and an airfoil with larger curvature near the shock wave location can improve the robustness in pitching moment against the variation of flight Mach number.

INTRODUCTION

The exploration of various planets in the solar system has been an academically interesting and attractive research topic in space science field because it may provide an important clue for understanding physical and biological early histories of the solar system evolution including the Earth. Especially, the Mars which is the nearest planet from the Earth is the most attractive target to be explored as the first step for understanding the whole solar system.

Conventional approaches to explore the Mars have been orbiting satellites around the Mars or rovers moving on the Martian surface. On the other hand, a Mars airplane has recently been expected as a new approach to explore Mars providing higher resolution power than the orbiting satellites and larger spatial coverage than the rovers. In addition, the Mars airplane is a challenging approach in engineering viewpoint.

One of the important issues in designing Mars airplanes is the uniqueness of these flight conditions. Compared to typical commercial Earth airplanes, the Mars airplanes are required to fly at lower Reynolds number condition (about 10^5 based on the wing root chord length of 1 m) due to thinner Martian atmosphere (about 1/100 of Earth's one)[1] and smaller airplane size such that the airplane can be stored into an aeroshell delivered by a launcher. In addition, those are required to fly at higher subsonic Mach number condition (more than 0.45) due to lower Martian speed of sound (about 2/3 of Earth's one). No airplane has ever flown at such unique conditions on the Earth except for high-altitude airplanes, therefore no design concept for Mars airplanes has been established sufficiently yet. Several airplanes have been already reported by many researches,[2–4] however, these airplanes were designed only based on existing design concepts for typical Earth airplanes. Therefore, it is required to search for better design of Mars airplane at low Reynolds number and high subsonic Mach number conditions in wide design space and establish new design concepts for future Mars airplane.

Another important issue of designing Mars airplanes is large Martian wind variations. It is well known that strong gradient winds (westerlies) blow over the Mars and these speeds have large daily and seasonal variations.[5] In addition, it is known that vertical winds induced by the so-called forced planetary wave blow over the Mars due to the interaction between the westerlies and hardly undulating Martian surface with mountains and craters,[6] too. The past studies of Mars airplanes,[2–4] however, considered the performance at

*Research Fellow, Institute of Fluid Science, 2-1-1 Katahira, Aoba-ku

†Research Associate, Institute of Space and Astronautical Science, 3-1-1 Yoshinodai

‡Professor, Institute of Space and Astronautical Science, 3-1-1 Yoshinodai

design point and ignored the effects of such wind variations. Martian wind variations may lead to large variations of flight conditions and drastic deterioration in performance of a Mars airplane, and thus failure in expected Mars exploratory mission. Therefore, it is also required to consider not only the performance at design point but also robustness of performance against the Martian wind variations in the design of Mars airplane.

Objectives of this paper are to search for airfoil designs of Mars airplane with robust characteristics of aerodynamic performance against Martian wind variations in wide design space by carrying out robust design optimizations coupled with the computational fluid dynamics (CFD) simulations, and to suggest new airfoil design information about the improvement in both optimality and robustness of aerodynamic performance against the wind variations for future Mars airplane. In this paper, two robust aerodynamic airfoil design optimizations are performed; the optimization considering robustness of lift to drag ratio against the variation of flight Mach number, and that considering robustness of pitching moment.

DEFINITION OF DESIGN PROBLEMS

The cruising flight condition of NASA's "Airplane for Mars Exploration (AME)"[2] is adopted as the present design point; Reynolds number based on root chord length $Re = 1.0 \times 10^5$, freestream Mach number $M_\infty = 0.4735$, and the angle of attack $\alpha = 2.0$ [deg]. In addition, it is assumed that M_∞ disperses around the design point of 0.4735 with its standard deviation of 0.1. Here, the value of 0.1 as the standard deviation of M_∞ is nearly equal to the daily and seasonal variations of westerly speeds of about 22 m/s at the altitude of several kilometers over the Mars,[5] where the Mars airplane is assumed to fly. In this study, two robust aerodynamic airfoil design optimizations for future Mars airplane are carried out; Case 1: considering robustness of lift to drag ratio L/D (L is lift and D is drag), and Case 2: considering robustness of pitching moment coefficient $C_{Mp} = M_p/(\frac{1}{2}\rho_\infty {u_\infty}^2 S_{ref} c_{ref})$ (M_p is pitching moment around 25 % chord position, ρ_∞ is freestream density, u_∞ is freestream velocity, S_{ref} is the wing area and c_{ref} is the root chord length), as follows:

- Case 1: considering robustness of L/D

  When M_∞ disperses around 0.4735 with its standard deviation of 0.1,

  - Maximize: mean value of L/D
  - Mimimize: standard deviation of L/D

- Case 2: considering robustness of C_{Mp}

  When M_∞ disperses around 0.4735 with its standard deviation of 0.1,

Fig. 1 NASA's "Airplane for Mars Exploration (AME)."[2]

  - Maximize: mean value of L/D
  - Maximize: sigma level satisfying $|C_{Mp}| \leq 0.13$

    ("sigma level" corresponds to probability of satisfying a constraint, referred to Ref. 7)

  and when $M_\infty = 0.4735$,

  - Subject to: $|C_{Mp}| \leq 0.13$

Case 1 aims at finding the airfoil configuration which can avoid failure in flying over an expected range, and Case 2 aims at finding one which can avoid failure in controlling pitching motion by its horizontal tail wing with $|C_{Mp}| = 0.13$ when the flight Mach number disperses widely around its design point. The structural constraint on airfoil thickness is not considered because we want to discuss an aerodynamic effect purely in the present study.

In both cases, airfoil configuration is defined by the B-spline curves with three fixed points corresponding to the leading and trailing edges and six control points whose coordinates can be specified flexibly, as shown in Fig. 2 (here, c is the airfoil chord length). The design variables are chordwise (x) and vertical (y) coordinates of the six control points, therefore the number of design variables is twelve. Such definition based on the B-spline curves has some advantages; the second-order derivative of coordinate along the B-spline curves is continuous, various airfoil configurations can be expressed, and definition of initial design space is intuitive.[8]

NUMERICAL METHODS

Optimizer

Design for multi-objective six sigma (DFMOSS)[7] is used as the present robust optimization approach. The DFMOSS has been newly developed by combining the ideas of design for six sigma (DFSS)[9] which is one of the conventional robust optimization approaches and

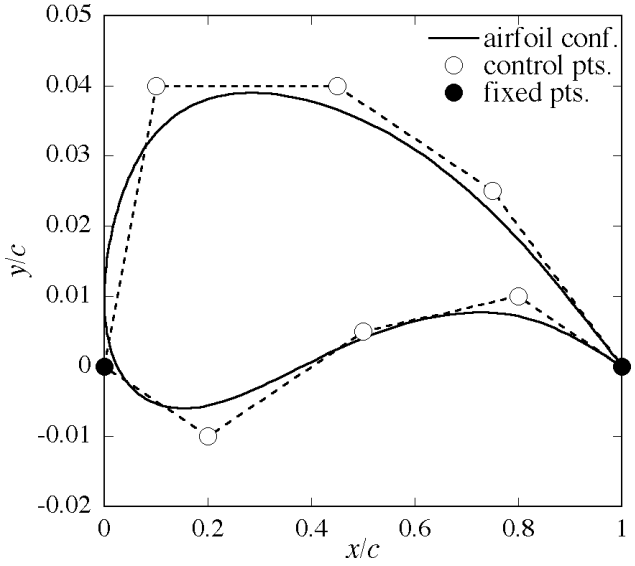

Fig. 2 Definition of airfoil configuration.

multi-objective evolutionary algorithm (MOEA).[10] In addition, the DFMOSS has some advantages, *e.g.*, it has no difficulty in pre-specifying input parameters before optimization, and trade-off information between optimality and robustness of performance which is useful design information for selecting one design from multiple design candidates according to designer's consideration can be obtained effectively by only one optimization run (details of DFMOSS are referred to Ref. 7).

The statistical values (mean value and standard deviation) of aerodynamic performance which are the present objective functions are estimated by the second-order Taylor's series expansion approach. Fitness values are evaluated by using a Pareto-ranking method,[11] a fitness sharing,[10,11] and the Michaleswicz's nonlinear function,[12] and constraints are dealt with by using the Pareto-optimality-based constraint-handling (PBCH) technique.[13] Parents are selected by the stochastic universal sampling (SUS).[14] Children are reproduced by the blended crossover (BLX-0.5) method[15] and uniform mutation[10] with a rate of 20 % and maximum perturbation range of 10 % of the design space. The alternation of generations is performed by the best-N selection.[16,17] Population size and number of generations are 64 and 100, respectively.

Evaluator of Aerodynamic Performance

Aerodynamic performance of an airfoil is evaluated by the computational fluid dynamics (CFD) simulation. The governing equations for the CFD simulation are two-dimensional Farve-averaged compressible thin-layer Navier-Stokes equations. The LU-ADI factorization algorithm[18] is used for the time integration. The inviscid terms of numerical fluxes are evaluated by the SHUS scheme.[19] In the inviscid terms, high-order accuracy is obtained by the third-order upwind-biased

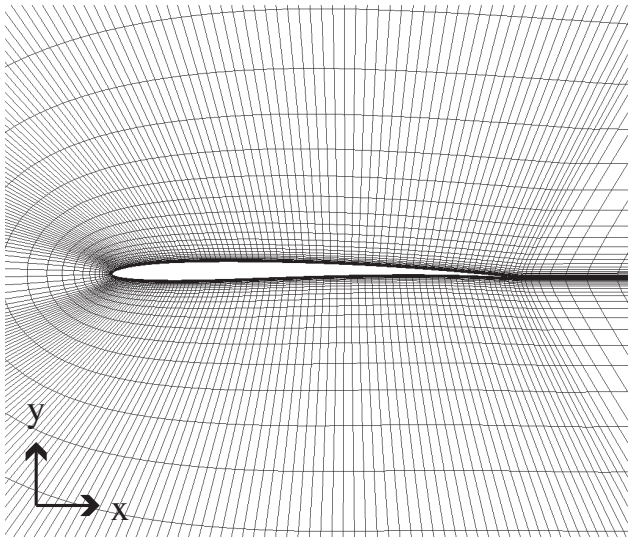

Fig. 3 Grid distribution.

MUSCL interpolation[20] based on the primitive variables with van Albada differentiable limiter.[21] The viscous terms are evaluated by the second-order central differencing, and the turbulent viscosity is modeled by the Baldwin-Lomax algebraic turbulence model.[22]

In the present study, C type grid as shown in Fig. 3 is used. The number of grid points is 251 in the direction around the airfoil (211 points over the airfoil surface), 51 in the direction normal to the airfoil surface, and the total number of grid points is 12,801. If flowfields around an airfoil are assumed to be laminar and simulated by using such number of grid points, unpractical vortices may occur and lead to misevaluation of aerodynamic performance. It is the reason why the present flowfields are assumed to be fully-turbulent by using the turbulence model.

Simulation Hardware

The computation time required for one evaluation of aerodynamic performance of airfoil using the CFD simulation is about five minutes with one processor of NEC SX-6 computing system owned by the Institute of Space and Astronautical Science (ISAS) of Japan Aerospace Exploration Agency (JAXA). In the present study, the optimizer distributes the multiple evaluators corresponding to the multiple design candidates of DFMOSS into 32 processors of this computing system in parallel. Therefore, the total computation time required for one present robust aerodynamic design optimization using DFMOSS can be reduced to about 56 hours.

RESULTS

Case 1: Considering Robustness of Lift to Drag Ratio

Figure 4 compares the optimal solution distribution (standard deviation of L/D against mean value of L/D) obtained by the present robust optimization in Case 1 with the optimal solution obtained by con-

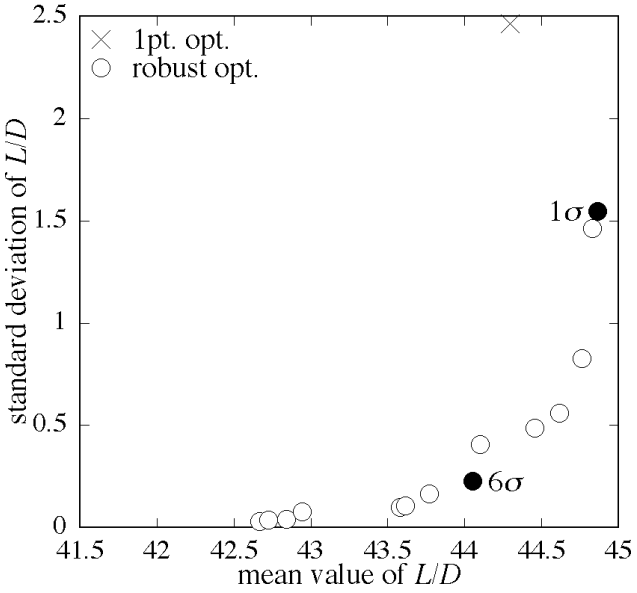

Fig. 4 Comparison of one-point optimal and robust optimal solutions in Case 1.

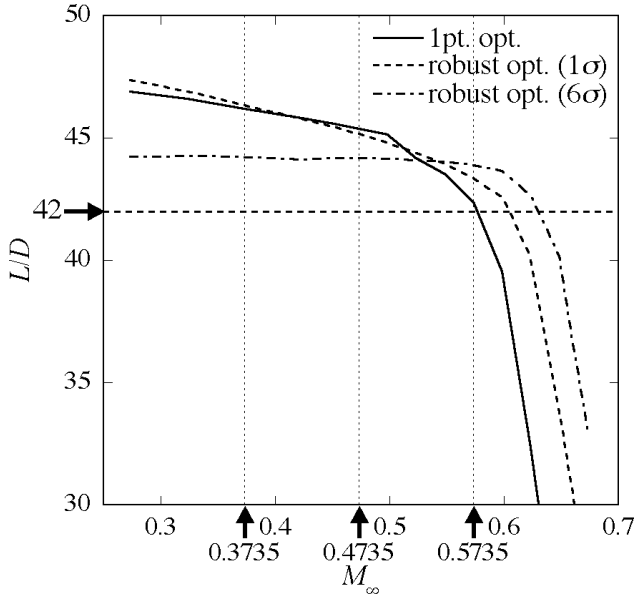

Fig. 5 L/D histories against M_∞ of one-point optimal and robust optimal solutions in Case 1.

ventional one-point optimization without considering robustness (only maximizing L/D at $M_\infty = 0.4735$). The one-point optimal solution has very large standard deviation of L/D This solution corresponds to the design with bad robustness quality of L/D against the variations of M_∞. On the other hand, the present robust optimization found total eighteen solutions with smaller standard deviations of L/D, i.e., better robustness qualities of L/D against the variations of M_∞ than the one-point optimal solution. These results prove necessity of not conventional optimization considering only optimality of performance but new optimization considering both optimality and robustness of performance for airfoil design realizing robust aerodynamic characteristics. In addition, detailed trade-off information between optimality and robustness can be understood easily from the obtained robust optimal solution distribution; *e.g.*, the standard deviation of L/D increases (robustness of L/D becomes worse) as the mean value of L/D increases (optimality of L/D becomes better), and its standard deviation increases drastically at its mean value of 44.5.

Hereafter, in Case 1, the one-point optimal solution and two robust optimal solutions whose sigma levels satisfying $L/D \geq 42$ are 1σ and 6σ, respectively, are compared and discussed. Here, the robust optimal solution with larger sigma level indicates the solution with more robust characteristic in terms of higher probability of satisfying $L/D \geq 42$, i.e., Mars airplane's flying an expected range safely when M_∞ disperses widely. Figure 5 shows the histories of L/D against M_∞ at $\alpha = 2.0$ [deg] of the one-point optimal solution and the robust optimal solutions with 1σ and 6σ robustness qualities. In the one-point optimal solution, L/D decreases drastically with an increment in M_∞, and it falls below its lower specification limit of 42 at high M_∞. On the other hand, the robust optimal solution with larger sigma level of L/D has slightly smaller L/D at the design point $M_\infty = 0.4735$, but more stable characteristics keeping large L/D against the increment in M_∞. This is because there is a more significant reduction in drag divergence against the increment in M_∞ when the sigma level of L/D becomes larger.

Figire 6 shows the airfoil configurations of the one-point optimal solution and the robust optimal solutions with 1σ and 6σ robustness qualities. In all these solutions, airfoils are very thin due to production of large difference in pressure between upper and lower surfaces, which leads to large lift. This is because friction drag is dominant and eventually the maximization of L/D can do nothing but increase lift in low Reynolds number flow around a Mars airplane. The one-point optimal solution has an airfoil with large maximum camber to generate strong expansion region without separation over the upper surface. On the other hand, the robust optimal solution with larger sigma level of L/D has an airfoil with smaller maximum camber.

Figure 7 compares the chordwise pressure coefficient $C_p = (p - p_\infty)/(\frac{1}{2}\rho_\infty {u_\infty}^2)$ (p is local pressure and p_∞ is freestream pressure) distributions over the airfoil surface at various M_∞ and at $\alpha = 2.0$ [deg] of robust optimal solutions with 1σ and 6σ robustness qualities. In the robust optimal solution with 1σ robustness quality as shown in Fig. 7(a), suction peak over the upper surface becomes stronger drastically with the increment in M_∞. Compared to this solution, the robust optimal solutions with 6σ robustness quality as shown in Fig. 7(b) has more moderate change of suction peak strength against the increment in M_∞. These results are owed to the result that a robust optimal solution

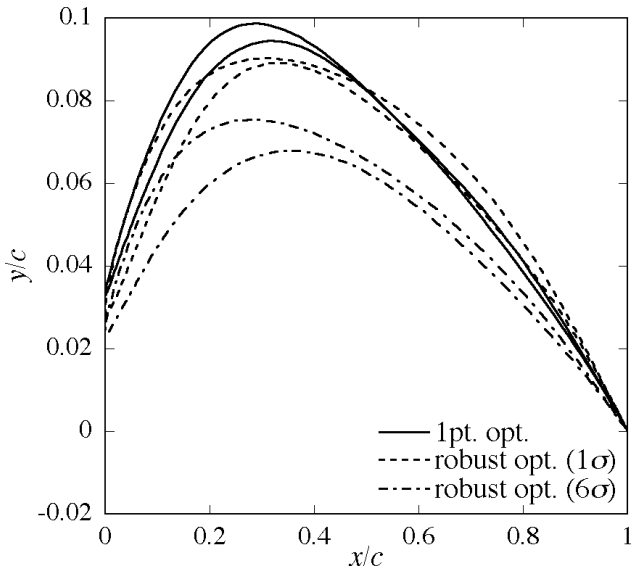

Fig. 6 Airfoil configurations of one-point optimal and robust optimal solutions in Case 1.

with larger sigma level of L/D has an airfoil with smaller maximum camber as shown in Fig. 6. Such airfoil can suppress the growth of shock wave and realize smaller increment in pressure drag (wave drag), and results in smaller decrement in lift to drag ratio against the increment in flight Mach number.

Case 2: Considering Robustness of Pitching Moment

Figure 8 compares the optimal solution distribution (sigma level satisfying $|C_{Mp}| \leq 0.13$ against mean value of L/D) obtained by the present robust optimization in Case 2 with the optimal solution obtained by conventional one-point optimization without considering robustness (only maximizing L/D subject to $|C_{Mp}| \leq 0.13$ at $M_\infty = 0.4735$). The one-point optimal solution has very small sigma level of 0σ satisfying $|C_{Mp}| \leq 0.13$, corresponding to the design with bad robustness quality of C_Mp against tha variations of M_∞. On the other hand, the present robust optimization found total forty solutions with larger sigma level satisfying $|C_{Mp}| \leq 0.13$, i.e., better robustness qualities of C_{Mp} against the variations of M_∞ than the one-point optimal solution. Similar to Case 1, these results prove necessity of not conventional optimization considering only optimality of performance but new optimization considering both optimality and robustness of performance for airfoil design realizing robust aerodynamic characteristics, too. In addition, the obtained robust optimal solution distribution revealed strong trade-off relation that the sigma level satisfying $|C_{Mp}| \leq 0.13$ decreases (robustness of C_{Mp} becomes worse) as the mean value of L/D increases (optimality of L/D becomes better).

Hereafter, in Case 2, the one-point optimal solution and two robust optimal solutions whose sigma levels satisfying $|C_{Mp}| \leq 0.13$ are 1σ and 8σ, respectively, are compared and discussed. Figure 9 shows the his-

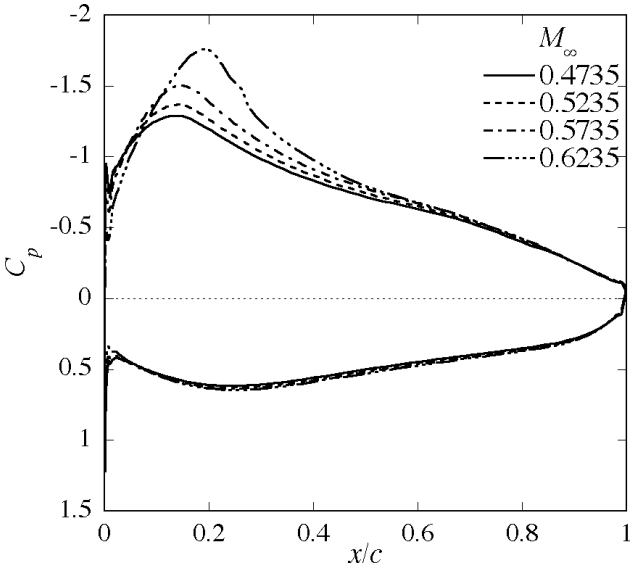

a) Robust optimal solution with 1σ.

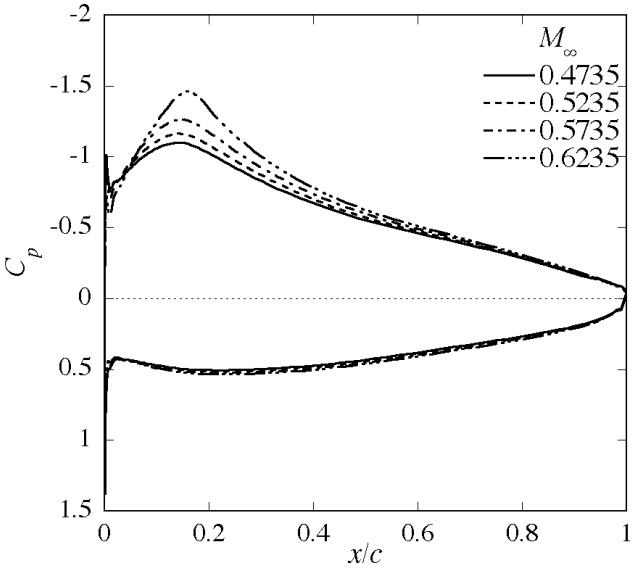

b) Robust optimal solution with 6σ.

Fig. 7 Chordwise C_p distributions over the airfoil surface at various M_∞ in Case 1.

tories of C_{Mp} against M_∞ at $\alpha = 2.0$ [deg] of the one-point optimal solution and the robust optimal solutions with 1σ and 8σ robustness qualities. In the one-point optimal solution, the constraint $|C_{Mp}| \leq 0.13$ is satisfied at the design point $M_\infty = 0.4735$. However, C_{Mp} falls below its lower specification limit of -0.13 and the constraint is not satisfied at M_∞ higher than 0.4735. In the robust optimal solution with larger sigma level satisfying $|C_{Mp}| \leq 0.13$, on the other hand, C_{Mp} history against M_∞ shifts higher from the lower limit of -0.13 and the constraint is satisfied until higher M_∞. In addition, the robust optimal solution with larger sigma level satisfying $|C_{Mp}| \leq 0.13$ has slightly smaller decrement in C_{Mp} against the increment in M_∞.

Figure 10 shows the airfoil configurations of the

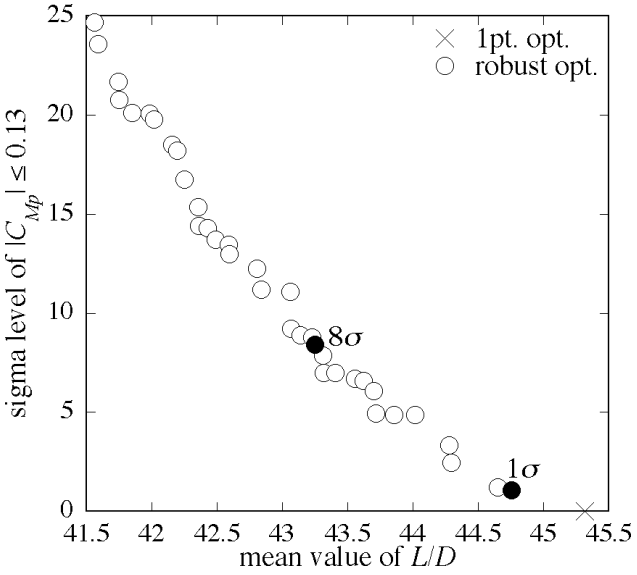

Fig. 8 Comparison of one-point optimal and robust optimal solutions in Case 2.

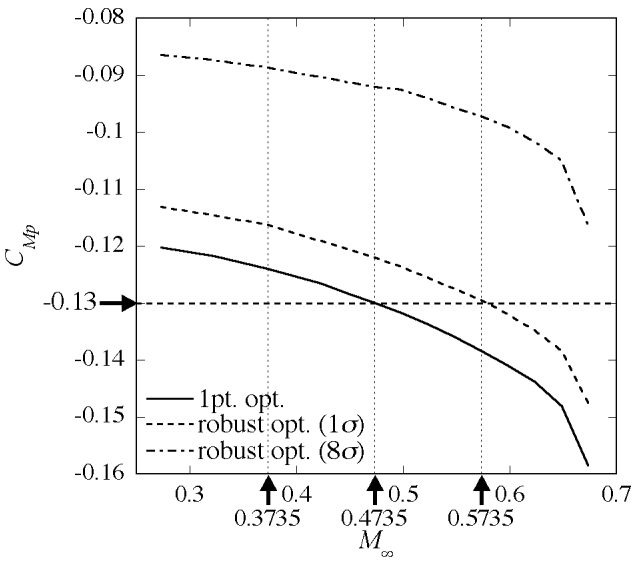

Fig. 9 C_{Mp} histories against M_∞ of one-point optimal and robust optimal solutions in Case 2.

one-point optimal solution and the robust optimal solutions with 1σ and 8σ robustness qualities. Similar to Case 1, all solutions have airfoils with very thin due to production of large lift. The one-point optimal solution and the robust optimal solution with 1σ robustness quality have airfoils with large maximum camber to generate strong expansion region without separation over the upper surface. On the other hand, the robust optimal solution with 8σ robustness quality has an airfoil folded down at the front part (about 15 % chord position). In addition, this fold becomes greater as the sigma level satisfying $|C_{Mp}| \leq 0.13$ becomes larger.

Figure 11 compares the chordwise C_p distributions over the airfoil surface at various M_∞ and at $\alpha = 2.0$ [deg] of robust optimal solutions with 1σ and 8σ ro-

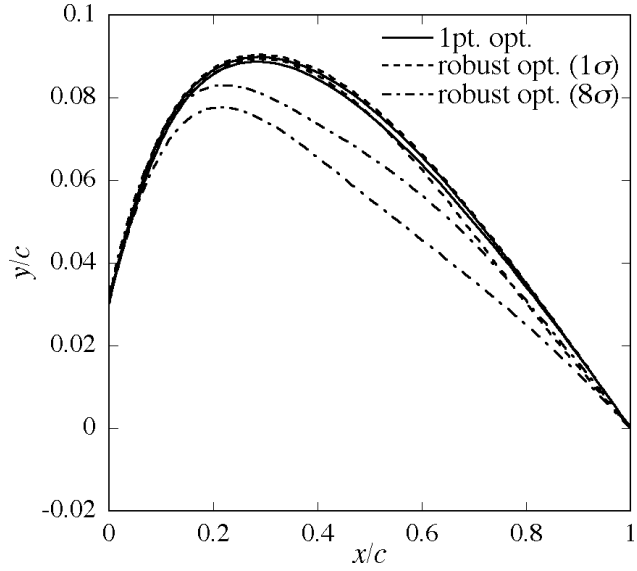

Fig. 10 Airfoil configurations of one-point optimal and robust optimal solutions in Case 2.

bustness qualities. In the robust optimal solution with 1σ robustness quality as shown in Fig. 11(a), suction peak over the upper surface moves backward with the increment in M_∞. Compared to this solution, the robust optimal solutions with 8σ robustness quality as shown in Fig. 11(b) has more moderate backward movement of suction peak against the increment in M_∞. These results are owed to the result that a robust optimal solution with larger sigma level satisfying $|C_{Mp}| \leq 0.13$ has an airfoil with larger curvature at the shock wave location as shown in Fig. 10. Such airfoil can suppress the backward movement of suction peak (shock wave) and results in smaller change in violation of the constraint $|C_{Mp}| \leq 0.13$.

CONCLUDING REMARKS

In this paper, robust aerodynamic airfoil design optimizations against wind variations for Mars exploratory airplane have been carried out by using DFMOSS coupled with the CFD simulation. The present robust optimization considering both optimality and robustness of performance successfully found the airfoil design with robust characteristic of aerodynamic performance against wind variations, while conventional optimization considering only optimality of performance cannot find such robust airfoil design. These results indicate importance of robust optimization for more reliable airfoil designs considering actual wind variations. In addition, the present robust aerodynamic airfoil design optimizations revealed detailed airfoil design information about the improvement in both optimality and robustness of aerodynamic performances against wind variations for future Mars airplane; an airfoil with smaller camber can improve the robustness in lift to drag ratio against the variation of flight Mach number, and an airfoil with larger curvature near the shock wave location can improve the

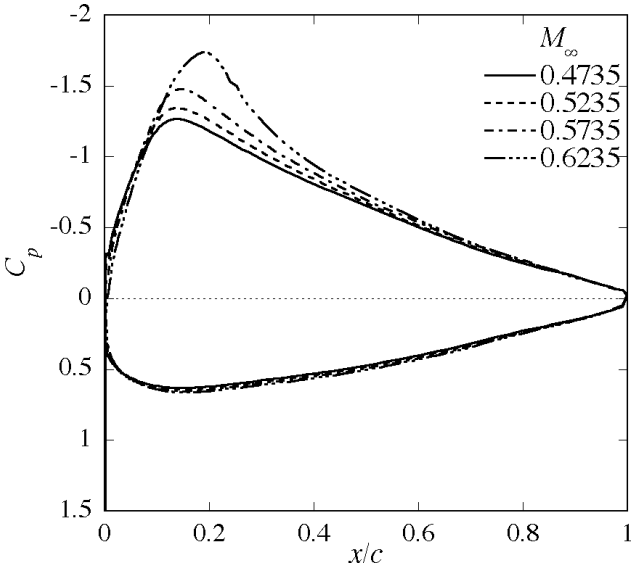

a) Robust optimal solution with 1σ.

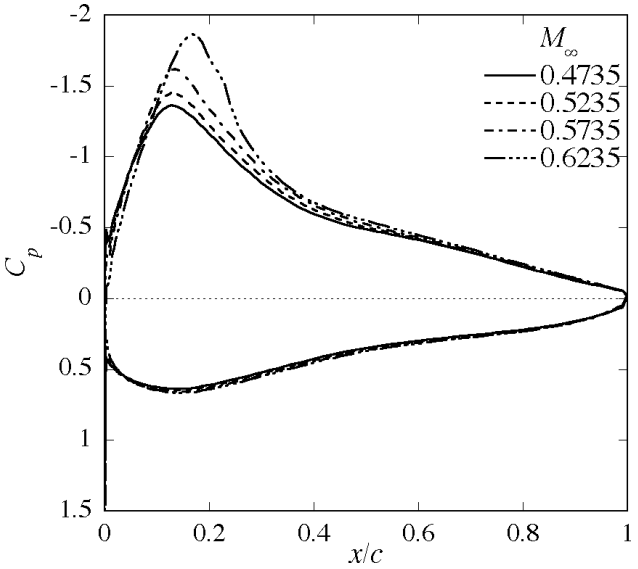

b) Robust optimal solution with 8σ.

Fig. 11 Chordwise C_p distributions over the airfoil surface at various M_∞ in Case 2.

robustness in pitching moment against the variation of flight Mach number.

References

[1]Matsuda, Y., *Planetary Meteorology*, University of Tokyo Press, Tokyo, 2000, in Japanese.

[2]Hall, D. W., Parks, R. W., and Morris, S., "Airplane for Mars Exploration," Tech. rep., NASA Ames Research Center, Moffett Federal Airfield, California, May 1997, URL: `http://www.redpeace.org/final_report.pdf`.

[3]Guynn, M. D., Croom, M. A., Smith, S. C., Parks, R. W., and Gelhausen, P. A., "Evolution of a Mars Airplane Concept for the ARES Mars Scout Mission," AIAA Paper 2003–6578, September 2003.

[4]Tanaka, Y., Okabe, Y., Suzuki, H., Nakamura, K., Kubo, D., Tokuhiro, M., and Rinoie, K., "Conceptual Design of Mars Airplane for Geographical Exploration," *Proceedings of the 36th JSASS Annual Meeting*, Tokyo, April 2005, pp. 61–64, in Japanese.

[5]Smith, M. D., Pearl, J. C., Conrath, B. J., and Christensen, P. R., "Thermal Emission Spectrometer Results: Mars Atmospheric Thermal Structure and Aerosol Distribution," *Journal of Geophysical Research*, Vol. 106, No. E10, October 2001, pp. 23929–23945.

[6]Hirota, I., *Global Meteorology*, University of Tokyo Press, Tokyo, 1992, in Japanese.

[7]Shimoyama, K., Oyama, A., and Fujii, K., "A New Efficient and Useful Robust Optimization Approach – Design for Multi-Objective Six Sigma," *Proceedings of the 2005 IEEE Congress on Evolutionary Computation*, Vol. 1, Edinburgh, September 2005, pp. 950–957.

[8]Oyama, A., Obayashi, S., Nakahashi, K., and Hirose, N., "Fractional Factorial Design of Genetic Coding for Aerodynamic Optimization," AIAA Paper 99–3298, June–July 1999.

[9]*iSIGHT Reference Guide Version 7.1*, Engineous Software, Inc., 2002, pp. 220–233.

[10]Deb, K., *Multi-Objective Optimization using Evolutionary Algorithms*, John Wiley & Sons, Ltd., Chichester, 2001.

[11]Fonseca, C. M. and Fleming, P. J., "Genetic Algorithms for Multiobjective Optimization: Formulation, Discussion and Generalization," *Proceedings of the 5th International Conference on Genetic Algorithms*, Morgan Kaufmann Publishers, Inc., San Mateo, California, 1993, pp. 416–423.

[12]Michalewicz, Z., *Genetic Algorithms + Data Structure = Evolution Programs*, Springer-Verlag, Berlin Heidelberg New York, 3rd, Revised and Extended ed., 1996.

[13]Oyama, A., Shimoyama, K., and Fujii, K., "New Constraint-Handling Method for Multi-Objective Multi-Constraint Evolutionary Optimization and Its Application to Space Plane Design," *EUROGEN 2005*, edited by R. Schilling, W. Hasse, J. Periaux, H. Baier, and G. Bugeda, FLM, Munich, September 2005.

[14]Baker, J. E., "Reducing Bias and Inefficiency in the Selection Algorithm," *Proceedings of the 2nd International Conference on Genetic Algorithms*, Morgan Kaufmann Publishers, Inc., San Mateo, California, 1987, pp. 41–49.

[15]Eshelman, L. J. and Schaffer, J. D., "Real-coded Genetic Algorithms and Interval Schemata," *Foundations of Genetic Algorithms 2*, Morgan Kaufmann Publishers, Inc., San Mateo, California, 1993, pp. 187–202.

[16]Eshelman, L. J., "The CHC Adaptive Search Algorithm: How to Have Safe When Engaging in Nontraditional Genetic Recombination," *Foundations of Genetic Algorithms*, Morgan Kaufmann Publishers, Inc., San Mateo, California, 1991, pp. 265–283.

[17]Tsutsui, S. and Fujimoto, Y., "Forking Genetic Algorithms with Blocking and Shrinking modes (fGA)," *Proceedings of the 5th International Conference on Genetic Algorithms*, Morgan Kaufmann Publishers, Inc., San Mateo, California, 1993, pp. 206–213.

[18]Fujii, K. and Obayashi, S., "Practical Applications of New LU-ADI Scheme for the Three-Dimensional Navier-Stokes Computation of Transonic Viscous Flows," AIAA Paper 86–0513, January 1986.

[19]Shima, E. and Jounouchi, T., "Role of CFD in Aeronautical Engineering (No. 14) –AUSM Type Upwind Schemes–," *Proceedings of the 14th NAL Symposium on Aircraft Computational Aerodynamics*, NAL SP–34, Tokyo, January 1997, pp. 7–12.

[20]van Leer, B., "Towards the Ultimate Conservation Difference Scheme. V. A Second-Order Sequel to Godunov's Method," *Journal of Computational Physics*, Vol. 32, 1979, pp. 101–136.

[21]Anderson, W. K., Thomas, J. L., and van Leer, B., "Comparison of Finite Volume Flux Vector Spllittings for the Euler Equations," *AIAA Journal*, Vol. 24, No. 9, September 1986, pp. 1453–1460.

[22]Baldwin, B. S. and Lomax, H., "Thin-Layer Approximation and Algebraic Model for Separated Turbulent Flows," AIAA Paper 78–257, January 1978.